# Chapter II: Review of Literatures

Over the years numerous works have been done on $TiO_2$ based materials in view of its various technological and application aspects. This chapter deals with the literatures related to magnetic, transport and ion irradiation based studies on $TiO_2$ and transition metal doped $TiO_2$. The relevant results on the magnetic and transport properties of $TiO_2$ as well as transition metal doped $TiO_2$ are discussed in Section 2.1 and Section 2.2 respectively. Effects of ion implantation/irradiation on structural and magnetic properties are depicted in Section 2.3. The discrepancies in the observed magnetism in these oxide systems are discussed in section 2.4.The objectives of the present thesis are outlined in Section 2.5.

## 2.1 Magnetic Properties

This section deals with the magnetic properties reported in $TiO_2$ as well as transition metal doped $TiO_2$. Section 2.1.1 gives a brief detail of the observed ferromagnetism in $TiO_2$ whereas Section 2.2.2 summarises the observed ferromagnetism in various transition metals like Co, Fe, Cr, V, Cu, Ni, Al, Nb and Mn doped $TiO_2$.

### 2.1.1Magnetism in $TiO_2$

Room temperature ferromagnetism (RTFM) in $TiO_2$ was first reported by Hong et al. (2006) and Yoon et al. (2006) in thin films deposited on $LaAlO_3$ substrate where the $T_c$ was far beyond the room temperature. Further, work in $TiO_2$ was followed by Ruamaiz et al. (2007) and Kim et al. (2009) where the observed ferromagnetism was solely ascribed to oxygen vacancies. Theoretically, Peng et al. (2009) suggested the formation Ti vacancy to cause ferromagnetism in $TiO_2$. These Ti vacancies are able to produce a net magnetic moment ~3.5 $\mu_B$ per vacancy whereas Ti divacancies also produce net magnetic moments of the magnitude ~2.05 $\mu_B$ per divacancy. When these two Ti vacancies secure the nearest sites, an $O_2$ dimer is supposed to form at the center of the divacancy that leads to a decrease in the total energy as well as in magnetic moment. Energetically, either Ti vacancies or divacancies favour the ferromagnetic order though it has not established experimentally. Yoon et al.

(2006) showed $T_C$ to be around 880 K for anatase $TiO_2$ film on $LaAlO_3$ (100) substrate using PLD technique and explained the magnetism on the basis of double exchange mechanism [Yoon et al. (2006)]. Mixed phase of anatase and rutile films grown on Si and quartz substrate showing ferromagnetism has been ascribed to creation of oxygen vacancies that leads to Stoner splitting of bands causing the ferromagnetic ordering [Rumaiz et al. (2007)]. The effect of annealing of $TiO_2$ films was found to decrease the magnetic moment and reducing the thickness has shown to enhance the same in $TiO_2$ rutile films deposited by spin coating and sputter deposition techniques on quartz and sapphire substrate, respectively [Sudakar et al. (2008)]. Ferromagnetism was triggered by the formation of $Ti^{3+}$-$V_O$ defect complex as reported by Xiang et al. (2013) in rutile $TiO_2$ single crystals under vacuum annealing [Dong-Xiang et al. (2013)]. The effect of anatase and rutile phase on magnetic properties of $TiO_2$ film deposited by sol-gel spin coating method on $Al_2O_3$ (0001) was studied by Kim et al. (2009). They have shown that $TiO_2$ in anatase has lower magnetic moment than in rutile phase. $TiO_2$ nanoparticles synthesized by sol-gel route showed higher magnetic moment under argon annealing [Ghosh et al. (2013)]. Rutile $TiO_2$ nanowires grown on Si (001) and glass substrates using solvothermal technique are shown to have higher saturation magnetisation ($M_s$) in comparison to Ni doped $TiO_2$ indicating magnetism originating from the surface defects like $Ti^{3+}$ and oxygen vacancies [Hoa et al. (2013)]. In case of rutile $TiO_2$ nanoparticles synthesized by chemical hydrolysis method, revealed magnetism originating from oxygen vacancies [Parras et al. (2013)]. $TiO_2$ pellets of rutile upon implantation of 4 MeV $Ar^{5+}$ ion demonstrated ferromagnetism at room temperature [Sanyal et al. (2014)]. Santara et al. showed oxygen vacancy mediated ferromagnetism in $TiO_2$ nanoribbons [Santara et al. (2014)]. Recently, using first-principles calculations, the coexistence of Ti vacancies and O vacancies are found to be responsible for the observed ferromagnetism. Calculations have shown that oxygen vacancy can induce local magnetic moments in $TiO_2$, however, the ferromagnetic exchange interaction of two vacancies is not strong enough to induce room-temperature

ferromagnetism on their own in $TiO_2$. The FM coupling between two Ti vacancies is about four times stronger than that between two oxygen vacancies which is found to be enhanced with the presence of oxygen vacancy. Basically, the electrons induced by oxygen vacancies mediate the long-range ferromagnetic exchange interaction between two distant Ti vacancies [Wang et al. (2014)]. Yang et al. (2010) showed theoretically, that a local magnetic moment of $1.0\mu_B$ per $Ti^{3+}$ in the lattice. The calculated results are in good agreement with the experimentally observed antiferromagnetic like behavior in oxygen-deficient Ti-O systems. The excess electrons introduced by an oxygen vacancy convert two $Ti^{4+}$ ions into two $Ti^{3+}$ ions and result in a local magnetic moment in anatase phase. However, the two $Ti^{3+}$ ions form a stable antiferromagnetic state. The trend is similar for oxygen-deficient rutile phase $TiO_2$. The calculated results are consistent with the experimentally observed antiferromagnetic behavior in oxygen-deficient Ti-O system [Yang et al. (2010)].

Not only in $TiO_2$, Sundaresan et al. (2006) reported the ferromagnetism as a universal feature of nanoparticles of inorganic oxides due to enhanced surface defects like oxygen vacancies. Similar unexpected ferromagnetism was also reported in $HfO_2$ thin films by Coey et al. (2005) which further strengthens the defect induced magnetism in these systems. To explain the magnetism in transition metal doped $TiO_2$, there are several models proposed in literature such as Ruderman-Kittel-Kasuya-Yosida (RKKY) model, Bound Magnetic Polaron (BMP) model, and Stoner type model as discussed in Chapter I. However, still no single mechanism could explain the observed ferromagnetism in these undoped oxide systems satisfactorily. Moreover, the most common feature in all these mechanisms is the vital role played by the interaction among the charge carriers and the magnetic moments that decisively control the electric as well as magnetic ordering in these oxide materials.

The ferromagnetism is considered to enhance in case of transition metal doping in $TiO_2$ host. The next section deals with the various transition metals doping in $TiO_2$ systems as reported in literatures.

### 2.1.2 Magnetism in Transition Metal Doped $TiO_2$

This section reviews the different reports available on transition metal (e.g., Co, Fe, Mn, Cr, Ni, Cu, Nb, and V) doped $TiO_2$.

**Co-doped $TiO_2$**

We have discussed here the studies on Co-doped $TiO_2$ DMS material in a chronological manner. Matsumoto et al. (2001) had reported ferromagnetism in Co-doped anatase $TiO_2$ thin films grown by a combinatorial pulsed laser deposition (PLD) and molecular beam epitaxy (MBE) technique which enhanced the ferromagnetic order upto 400 K having magnetic moment of 0.32 $\mu_B$/Co for 7 at.% Co (Fig. 2.1(a), prior to the discovery of ferromagnetism in Mn doped ZnO [Sharma et al. (2003)]. Soon after, Chambers et al. (2001) showed the enhanced ferromagnetic moment upto 1.26 $\mu_B$/Co in oxygen plasma assisted (OPA) MBE film with relatively lower Co concentration (Co~3 at%) (Fig.2.1(b)) [Chambers et al. (2001)].

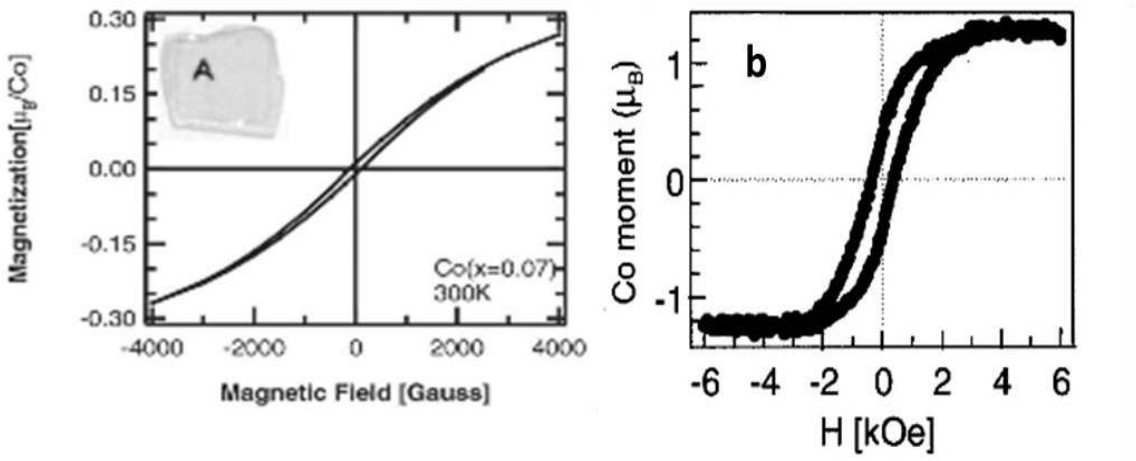


**Fig.2.1** Magnetisation as a function of applied magnetic field for (a) $Ti_{0.93}Co_{0.07}O_{2-\delta}$ film and [Matsumato et al. (2001)] (b) $Ti_{0.97}Co_{0.03}O_{2-\delta}$ film [After Chambers et al. (2001)]

The films showed ferromagnetism were of anatase phase only. After one year, Park et al. (2002) demonstrated ferromagnetism in Co-doped rutile films deposited by sputtering technique with enhancing the $T_C$ beyond 400 K. The magnetic moment was 0.94 $\mu_B$ /Co for Co concentration ~6 at.% which was less than the moment reported in anatase phase [Park et al. (2002)]. Shim et al.

(2002) observed decrease in magnetisation from 85 emu/cc to 32 emu/cc with increasing Co concentration from 1 to 9 at% [Shim et al. (2002)]. Later, Kim et al. found a variation in magnetic moment from 0.5 to 2.25 $\mu_B$ for 4 at% Co-doped anatase $TiO_2$ films deposited on $SrTiO_3$ (001) substrates by increasing the oxygen partial pressure from $1x10^{-7}$ to $1x10^{-4}$ Torr employing PLD technique [Kim et al. (2002)]. A relatively high magnetic moment of 4.1 $\mu_B$ was observed by Manivanan et al. (2003) in hydrogenated anatase Co-doped $TiO_2$ nanopartices without any signature of Co clustering. Kim et al. (2003) reported magnetic moment of 1.55 $\mu_B$ in anatase Co-doped $TiO_2$ (7 at.%) films deposited by laser molecular beam epitaxy on $LaAlO_3$ substrate. Similar to Park et al. (2002), Stampe et al. (2003) also observed the magnetic moment to be ~ 1.7 $\mu_B$ in case of anatase film deposited on $LaAlO_3$ substrate which was higher than the observed 0.6$\mu_B$ for rutile film deposited on $Al_2O_3$ substrate. Shinde et al. (2003) demonstrated ferromagnetism in 7 at.% Co-doped anatase film deposited on $SrTiO_3$ (001) substrate with a magnetic moment 1.4 $\mu_B$, lower than that of film deposited on $LaAlO_3$ substrate [Kim et al. (2003)]. Using a spray pyrolysis technique, Manivanan et al. (2003) obtained a magnetic moment of 3 $\mu_B$ for 10 at% Co-doped anatase films grown on glass substrate which is quite high. Clustering of Co was observed in Co implanted $TiO_2$ films giving rise to ferromagnetic order in films deposited on $SrTiO_3$ substrate with a magnetic moment ~1.7 $\mu_B$ [Kim et al. (2003)]. Similar clustering of Co was reported by Kennedy and Stampe (2003) with varying Co from 0.05 to 3.4 at.%. Hong et al. (2004) observed ferromagnetism in 12 at.% Co-doped $TiO_2$ films deposited on $LaAlO_3$ substrate [Hong et al. (2004)]. No change in saturation magnetisation in case of anatase Co-doped $TiO_2$ (0.5 $\mu_B$) nanoparticles with x = 0.5 and 0.1 was observed by Cho et al. (2004). A higher magnetic moment (4.2 $\mu_B$) closer to the bulk Co in high spin state was achieved by Bryan et al. [Bryan et al. (2004)].

Shinde et al. (2004) noticed the magnetic moment ~ 2 $\mu_B$ in rutile Co 2 at% doped $TiO_2$ films grown on R-$Al_2O_3$ substrate. Magnetic moment was found as 0.31 $\mu_B$ for rutile doped $TiO_2$ on Si substrate and 0.23 $\mu_B$ for anatase

$LaAlO_3$ substrate [Hong et al. (2004)]. Adopting rf-magnetron sputtering technique, Jeong et al. (2005) found the magnetic moment of 0.7 $\mu_B$ in anatase Co-doped film [Jeong et al. (2005)]. With same deposition technique, Griffin et al. (2005) demonstrated a magnetic moment of 1.1 $\mu_B$ for 2 at.% Co-doped $TiO_2$ film grown on $LaAlO_3$ substrate [Griffin et al. (2005)]. Roberts et al. (2008) studied the effect of ultra-high vacuum annealing of Co (~3 at.%) doped anatase $TiO_2$ films deposited on $LaAlO_3$ substrate by the aforementioned technique [Roberts et al. (2008)]. They claimed an increase in magnetic moment from 0.35 $\mu_B$ (as deposited) to 0.68 $\mu_B$ under the vacuum annealing condition.

Magnetic moment was further found to decrease from 0.74 to 0.02 $\mu_B$ (x = 0.026 to 0.312) for anatase as well as rutile films from 0.54 to 0.04 $\mu_B$ (x = 0.026 to 0.169) in case of Co-doped films using magnetron sputtering [Mi et al. (2009)]. A highest dopant percentage ~ 20 was reported by Osada et al. (2006) for Co-doped $TiO_2$ nanosheets deposited on quartz or Si substrate with a marginally less magnetic moment of 1.4 $\mu_B$. Suryananrayan et al. (2005) observed an increase in magnetic moment from 0.15 $\mu_B$ to 0.36 $\mu_B$ measured at 2000 Oe for the 3 at% Co-doped $TiO_2$ films deposited by sol-gel spin coating. For the same Co concentration, Fu et al. (2006) and Zhang et al. (2006) reported magnetic moment of 0.4 $\mu_B$ and 0.38 $\mu_B$, respectively having same anatase phase grown on $LaAlO_3$ substrate using PLD technique [Fu et al. (2006), Zhang et al. (2006)]. A quite low magnetic moment of 0.0066 $\mu_B$ was observed for doped anatase nanofibres that decrease to 0.0047 $\mu_B$ for rutile nanofibres grown by electrospinning method [Jia et al. (2007)]. Magnetic moment was also varied from 0.35 to 0.6 $\mu_B$, for films deposited by electrochemical deposition technique [Wang et al. (2007)]. Hu et al. (2008) demonstrated a magnetic moment of 1.75 $\mu_B$ in 7 at.% Co-doped rutile film deposited on c-sapphire substrate using PLD technique. On similar substrate, Fukumura et al. (2008) showed an increase in magnetic moment from 1.1 to 1.5 $\mu_B$ for Co 5 and 10 at.% respectively by MBE technique. In case of anatase nanoparticles synthesized by hydrothermal technique, Pereira et al. (2008)

showed an anomalous behaviour. With increase in Co concentration from 3 to 7 at.%, the magnetic moment was enhanced from 0.2 to 0.6 $\mu_B$. However, with further increase in Co concentration, the magnetic moment decreased from 0.4 to 0.1 $\mu_B$ [Pereira et al. (2008)]. A magnetic moment of 0.34 $\mu_B$ was observed by McClure et al. (2008) in the as grown thin film of Co-doped $TiO_2$ by liquid precursor metal organic chemical vapour deposition technique [McClure et al. (2008)]. However, after post annealing of the films, ferromagnetism was vanished [McClure (2008)]. Annealing of Co on $TiO_2$ rutile films led to a ferromagnetic moment of 0.9 $\mu_B$ [Yan et al. (2009)]. Yamasaki et al. (2009) observed a high magnetic moment of 3 $\mu_B$ in Co-doped $TiO_2$ films grown on glass substrate. By sol-gel spin coating method, magnetic moment was found to be ~1.8 $\mu_B$ for Co-doped films [Xu et al. (2010)]. A change in phase from anatase for Co 2.5 at% to anatase and rutile mixed phase for Co 10 at.% was observed with a subsequent increase in magnetic moment from 0.28 $\mu_B$ to 0.38 $\mu_B$ in case of spraypyrolyzed $TiO_2$ films grown on quartz substrate [Sharma et al. (2010)]. Effect of post annealing was discussed by Goh et al. (2011) for 5 at.% Co-doped $TiO_2$ films deposited on $SrTiO_3$ (001) substrate by liquid phase deposition method.

Singh et al. (2012) studied the ferromagnetism of cobalt doped anatase $TiO_2$ thin films using element specific XMCD at the Co $L_{2,3}$ edges in both the surface sensitive total electron yield (TEY) and bulk sensitive total fluorescence yield (TFY) modes. The large magnetic moment of the Co ions, 0.6-2.4 $\mu_B$/Co, was observed by the TFY method. The origin of ferromagnetism at room-temperature in anatase $Ti_{1-x}Co_xO_{2-\delta}$ was further supported by the XMCD study of the samples with different carrier concentration. They observed, the positions of $Co^{2+}$ atoms seem to be displaced from the regular $Ti^{4+}$ sites causing random crystal fields. The magnetic moment

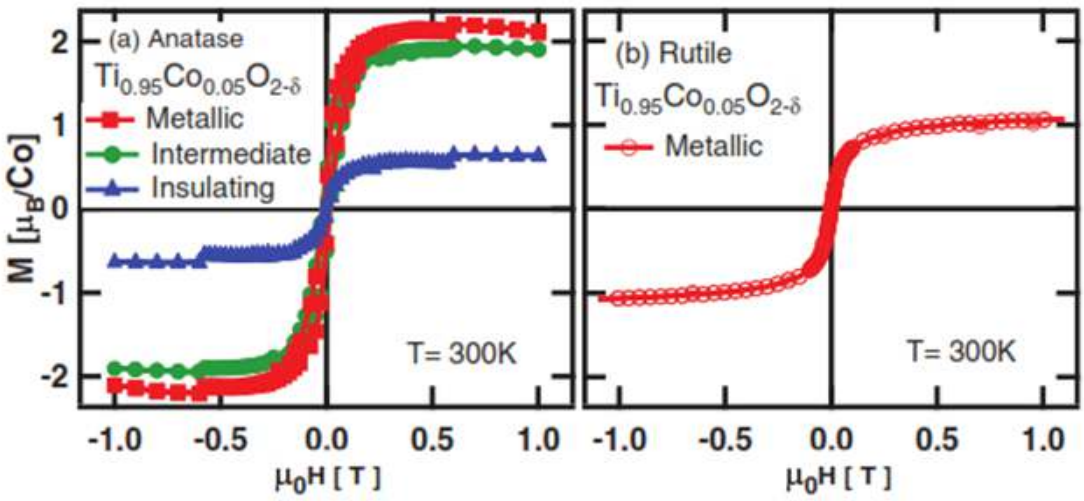


**Fig.2.2** M-H of $Ti_{0.95}Co_{0.05}O_{2-\delta}$ (a) Metallic, intermediate, and insulating anatase samples. (b) Metallic rutile sample [After Singh et al. (2012)]

values deduced with the TEY mode is found to be <0.31 $\mu_B$/Co, indicating the presence of a magnetically dead layer of ~5 nm thickness at the sample surfaces. The results showed anatase $Ti_{0.95}Co_{0.05}O_{2-\delta}$ in its metallic phase demonstrating higher magnetic moment than the insulating anatase and metallic rutile phase (Fig.2.2) [Singh et al. (2012)].

**Fe doped $TiO_2$**

In Fe doped rutile $TiO_2$, a negligible change in magnetisation from 2.3 to 2.4 $\mu_B$/Fe was observed by varying the Fe concentration from 0.02 to 0.08 in films grown on α-$Al_2O_3$ substrate [Wang et al. (2003)]. Anatase Fe doped $TiO_2$ nanoparticles prepared by chemical solution method showed magnetic moment ~0.067 $\mu_B$/Fe at an applied field of 1Tesla [Lee et al. (2004)]. However, Wang et al. (2005) showed paramagnetism in Fe doped $TiO_2$, with Fe upto 20 at% in anatase and rutile mixed phase powder samples prepared by oxidative pyrolysis method [Wang et al. (2005)]. The highest ever magnetic moment observed in Fe doped $TiO_2$ nanoparticles was 6.15 $\mu_B$/Fe for anatase doped nanoparticles synthesized by microemulsion technique [Rodriguez-Torres et al. (2008)]. Bapna et al. (2012) demonstrated ferromagnetism in 4 at.% Fe doped $TiO_2$ films on $LaAlO_3$ substrate by PLD technique. Suraynarayan et al. (2005) studied the role of vacuum annealing on Fe doped $TiO_2$ (Fe 0.05) films in both anatase and rutile forms deposited on c-axis oriented sapphire substrates. While

the magnetic moment of the as prepared anatase film was enhanced from 0.03 to 0.46 $\mu_B$/Fe, in case of rutile films, the magnetic moment was found to decrease from 0.09 to 0.014 $\mu_B$/Fe under vacuum annealing [Suryananrayan et al. (2005)]. Lee and Kim (2007) showed that magnetisation increase ten times (0.03 to 0.33 $\mu_B$/Fe) for Fe doped $TiO_2$ (x = 0.01) under vacuum annealing [Lee and Kim (2007)]. Further, Fan et al. (2008) observed the role of atmosphere on rutile ball milled powder samples. The Fe doped powder (Fe = 4.4 at.%) in air condition had shown the magnetic moment 0.015 $\mu_B$/Fe that decreased to 0.09 $\mu_B$/Fe in presence of $O_2$ [Lin et al. (2008)]. Upon annealing in oxygen atmosphere, Bapna et al. observed a decrease in magnetisation as a signature of annealing of oxygen vacancies [Bapna et al. (2012)]. In high energy ball milled rutile powders of Fe doped $TiO_2$ (Fe = 0.04), the magnetic moment was found to be ~ 0.15 $\mu_B$/Fe [Xiaoyan et al. (2006)]. For Fe doped anatase $TiO_2$ nanoparticles with Fe < 2 at.%, ferromagnetism was observed [Zhu et al. (2007)]. Rutile nanorods of Fe doped $TiO_2$ for Fe concentration ~ 3 at.% demonstrated ferromagnetism at room temperature [Melghit and Bouziane (2008)]. A robust magnetic moment ~3.7 $\mu_B$/Fe was found for anatase Fe doped $TiO_2$ films with 15 at.% of Fe deposited by reactive magnetron sputtering [Meng et al. (2007)]. Recently, Santara et al. (2014) explained the ferromagnetism in Fe doped $TiO_2$ nanoribbons according to BMP model that include an electron locally trapped by an oxygen vacancy. With the trapped electron occupying an orbital overlapping with the unpaired electron ($3d^1$) of a $Ti^{3+}$ ion and/or the unpaired electron ($3d^5$) of a $Fe^{3+}$ ion is found to be responsible for the ferromagnetic order [Santara et al. (2014)]. Similar BMP model has been used to explain the observed ferromagnetism in Fe doped $TiO_2$ nanopowders [Navarro et al. (2014)].

**Cr doped $TiO_2$**

Wang et al. (2004) reported ferromagnetism in 6 at.% Cr (antiferromagnetic) doped rutile $TiO_2$ deposited on R-plane sapphire substrate. With increasing Cr concentration, the saturation magnetisation decreased from 2.9 $\mu_B$ /Cr. The variation in magnetic moment was observed in anatase $TiO_2$

film deposited on LAO and STO substrates from 0.05 to 0.06 $\mu_B$/Cr [Kaspar et al. (2005)]. Annealing Cr doped $TiO_2$ amorphous films at 300 °C transformed them to anatase crystalline phase destroying the observed ferromagnetism with 0.321 $\mu_B$/Cr [Wang et al. (2006)]. Zhang et al. (2008) studied the role of oxygen partial pressure on Cr doped $TiO_2$ films deposited on glass and kapton substrate by co-sputtering method. By decreasing the oxygen pressure from 0 to 0.16 Pa, the magnetisation was found to decrease from 0.42 to 0.09 $\mu_B$/Cr, respectively for Cr ~ 0.05.

**Mn doped $TiO_2$**

Mn doped $TiO_2$ rutile films deposited on α-$Al_2O_3$ substrates by PLD technique showed ferromagnetism at room temperature [Wang et al. (2004)]. With increase in Mn concentration from 2 to 8 at.%, magnetic moment was increased from 0.65 to 0.83 $\mu_B$/Mn. Further increasing the Mn concentration to 12 at.%, reduced the magnetic moment to 0.14 $\mu_B$/Mn [Wang et al. (2004)]. On the contrary, Sharma et al. (2011) observed an increase in magnetic moment from 0.17 $\mu_B$ to 0.31 $\mu_B$/Mn with increase in Mn concentration from 0.10 to 0.05 [Sharma et al. (2011)]. Xu et al. (2006) explored the variation in magnetic moment with phase of 10 at.% Mn doped in $TiO_2$films deposited by sol-gel spin coating method. The magnetic moment was found to ~0.07 $\mu_B$/Mn for anatase phase whereas 1.1 $\mu_B$ /Mn for rutile [Xu et al. (2006)]. Further, the magnetic moment was increased from 0.75 to 1 $\mu_B$/Mn upon annealing [Xu et al. (2008)]

**Cu doped $TiO_2$**

Nonmagnetic Cu doped $TiO_2$ showed room temperature ferromagnetism [Duhalde et al. (2005), Zheng et al. (2014)]. Duhalde et al. demonstrated ferromagnetism in PLD grown films. The magnetic moment was found to be 1.5$\mu_B$ /Cu atom which is significantly large. Theoretical calculations suggest large magnetic moment can only be possible if an oxygen vacancy is situated in the nearest neighbor shell of Cu. It suggests the role of oxygen vacancies is crucial for the appearance of ferromagnetism. These oxygen vacancies are favoured by Cu doping [Duhalde et al. (2005)]. In addition, Zhang et al. (2014)

suggested the ferromagnetism in Cu doped anatase $TiO_2$ films is due to grain boundary defects.

The oxygen defects can be the dominating factor for increasing the saturation moment of these Cu-doped $TiO_2$ films. These results clearly suggest the important role of oxygen vacancies in driving the ferromagnetism [Zheng et al. (2014)]. Theoretically, Errico et al. (2005) studied the effect of oxygen vacancies on the ferromagnetic properties of $TiO_2$. Their presence was found to decrease the energy required to introduce the impurities in the host lattice and hence presence of impurities are related to a higher vacancy concentration.

**Ni doped $TiO_2$**

Hou et al. (2007) reported ferromagnetism in Ni doped anatase $TiO_2$ (x = 0.02, 0.04, 0.06, 0.08) deposited on $SiO_2$ by reactive magnetron sputtering. With increase in Ni concentration, saturation magnetisation was increased. The saturation magnetisation was found between 0.61 to 1.0 $\mu_B$/Ni for $O_2$ annealing and 0.67 to 1.28 $\mu_B$/Ni for Ar annealing condition. So, it is evident that annealing under oxygen deficient/reducing condition (annealing under Ar), leads to formation of oxygen vacancies that increases the ferromagnetic moment [Hou et al. (2007)]. Cho et al. (2006) observed ferromagnetism in Ni doped $TiO_2$ by sol-gel method for Ni concentration 1 to 8 at.% [Cho et al. (2006)].

**V doped $TiO_2$**

A high magnetic moment ~4.23 $\mu_B$/V was reported by Hong et al. (2004) in V (5 at%) doped $TiO_2$ film deposited on $LaAlO_3$ substrate. Tian et al. (2008) demonstrated ferromagnetism in V doped $TiO_2$ nanoparticles in anatase form synthesized by sol-gel technique with x = 0 to 0.16.

**Al doped $TiO_2$**

Wang et al. (2014) demonstrated ferromagnetism in Al doped rutile $TiO_2$ thin films grown on $Al_2O_3$ substrates by PLD technique with $T_c$ near 340 K. The $M_s$ was found to be 0.68, 0.78 and 0.33 $\mu_B / V$ for 2, 6 and 8 at.% Al, respectively. Magnetic moment associated with the formation of $Ti^{3+}$ ions was found in all cases but they couple differently as a result showing different

magnetic moments. The magnetism is supposed to be associated with the electrons generated by the oxygen vacancy upon Al doping. The electron associated with the defect occupies nearby Ti sites leading to formation of $Ti^{3+}$ and at the same time, it spatially extend the wave functions assuring overlapping between neighbours that may the reason behind the room temperature ferromagnetism [Wang et al. (2014)].

**Nb doped $TiO_2$**

The magnetic effect was studied in nonmagnetic Nb (5 at%) doped $TiO_2$ thin films deposited by PLD. Instead of magnetic measurements, transport and magneto-transport measurements revealed the presence of magnetic moments in the system. The extrinsic factors for the ferromagnetism was discarded and suggested that doping nonmagnetic elements in a nonmagnetic host may tailor the material property which opens up new avenues for defect induced magnetism for the possible spintronics applications. [Zhang et al. (2009)].

**2.2 Transport Properties**

Electrical properties of $TiO_2$ thin films are found to differ significantly from anatase to rutile phase. Resistivity and Hall-effect measurements showed an insulator-metal transition in a donor band in anatase thin films with relatively high donor concentrations [Tang et al. (1994)]. However, for similar donor concentrations, transition was not observed in rutile thin films. It signifies a larger effective Bohr radius of donor electrons in anatase than in rutile consequently having a smaller electron effective mass. The smaller effective mass in anatase is consistent with the high mobility responsible for band like conduction. It is also responsible for the very shallow donor energies in anatase phase [Tang et al. (1994)].

Wang et al. (2003) investigated rutile $Fe_xTi_{1-x}O_{2-\delta}$ ($x$ = 0.02, 0.06, and 0.08) thin films grown on α-$Al_2O_3$ substrates by PLD [Wang et al. (2003)]. The temperature dependent resistivity was nearly metallic at room temperature but behaved like semiconducting at lower temperatures. The extraordinary Hall effect which is later termed as anomalous Hall effect, one of the key

characteristics of the ferromagnetic semiconductor with coercivities similar to the hysteresis curves in magnetic material was observed at room temperature [Fig.2.3]. The hysteresis signified the interaction of itinerant carriers and localized electron spins of Fe ions. The carriers were found to be of *p* type with a carrier density of about $10^{22}/cm^3$, [Wang et al. (2003)]. The magneto-resistance (MR) was about to be 5% at 2 K (@5 T field) and it became negative (less than 0.1%) when measured at room temperature.

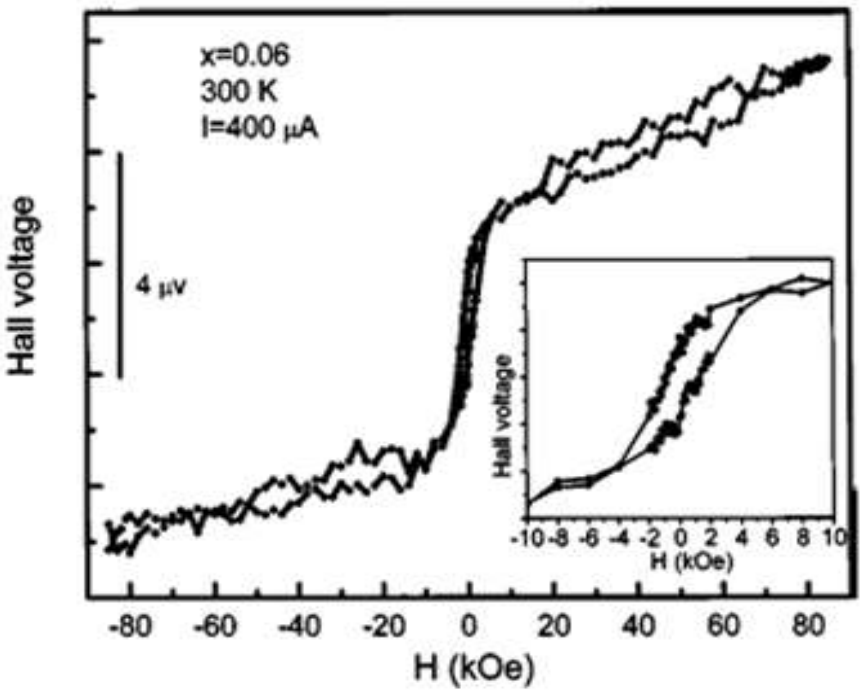


**Fig.2.3** Hall voltage versus applied magnetic field at 300 K for x = 0.06. The extraordinary Hall effect dominates at low fields and shows hysteretic behaviour as shown in the inset [After Wang et al. (2003)]

Shinde et al. (2003) reported the transport and magnetotransport properties of $TiO_2$ and $Ti_{0.99}Co_{0.01}O_{2-\delta}$ film. The Hall effect measurements showed n-type conduction in both films with estimated carrier concentrations of ~1.4 x $10^{18}$ and 2.1 x $10^{18}/cm^3$, respectively at 300 K. The conduction mechanism was suggested to be completely due to the presence of oxygen vacancies that introduce states just below the conduction band. The difference in resistivity of pure anatase $TiO_2$ caused by Co substitution may occur due to vacancy population to satisfy its valence ($Co^{2+}$) as well as its contribution to

magnetic scattering. Increase in resistivity in spite of an increase in carrier concentration suggests drop in mobility due to magnetic or strain scattering processes. The MR was found to be positive and is significant at low temperatures that correspond to conditions representing partial ionization of shallow donor states, commonly attributed to oxygen vacancies [Shinde et al. (2003)]. The ferromagnetism observed in these systems requires the confirmation of intrinsic nature of magnetism. Earlier it was believed that observation of anomalous Hall effect (AHE) confirms the intrinsic ferromagnetic behaviour [Shinde et al. (2004)]. However, Shinde et al. (2004) showed that even presence of clusters of Co nanoparticles in the Co-doped $TiO_2$ causes AHE. Hence, to conclude the intrinsic nature of the ferromagnetic ordering in DMS material, one needs to perform various characterization techniques to confirm the true magnetism in these systems.

In case of Co-doped anatase $TiO_2$ films, Ramaneti et al. demonstrated the conduction in a metallic donor-impurity band with a signature of the Kondo effect. The resistivity ρ, measured at room temperature was found to be ~ 1Ωcm for $TiO_2$ film whereas an order of magnitude smaller for Co-doped films. From Fig.2.4, it is clear that the low temperature ($T$) behavior of the doped films is completely different from the undoped ones. The inset of Fig.2.4 indicates for the $TiO_2$ films, ρ increases exponentially with $1/T$ as an indication of activated transport, whereas for Co-doped films, it remains comparatively constant and almost saturates at low temperature. The authors have also discarded the hopping transport mechanism in the films as previously reported in rutile samples containing Co metal clusters. However, the high Kondo temperature $T_K$ ~120 K suggests a strong interaction between Co spins and conduction electrons in the impurity band (an order of magnitude higher than observed value in metals) and implies conduction electrons and the Co local moments are in states that are energetically closer to have strong interaction. [Ramaneti et al. (2007)].

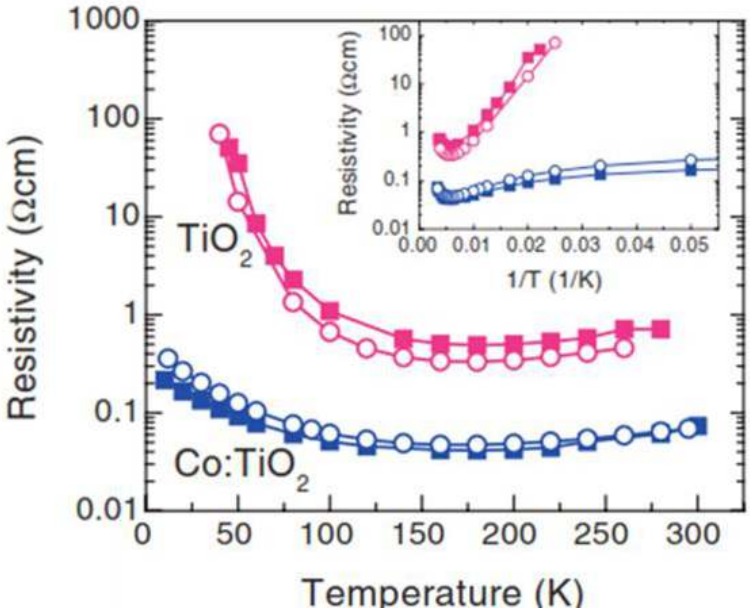


**Fig.2.4** Electrical properties of anatase $TiO_2$ and Co: $TiO_2$. The inset shows the resistivity versus 1/T of the anatase $TiO_2$ and Co: $TiO_2$. [After Ramaneti et al. (2007)]

Similar Kondo like behaviour was observed by Bapna et al. (2012) in case of $Ti_{1-x}Fe_xO_{2-\delta}$ (x = 0, 0.04) films deposited by PLD. They have showed a competition between the magnetic ordering mechanism by $J_{RKKY}$ and the moment screening mechanism by $J_{Kondo}$ in view of popular Doniach phase diagram [Ramaneti et al. (2007)]. The coupling between the local moment and the charge carriers is evidenced from magnetoresistance measurements of the films. Overall, the coupling of local magnetic moment and the spin of itinerant carriers opens new avenues for defect engineering by transition metal doping [Bapna et al. (2012)].

## 2.3 Low Energy Ion Implantation/ Swift Heavy Ion Irradiation Studies

### *Implantation in $TiO_2$*

Transition metals like Co [Akdogan et al. (2006), Kim et al. (2005), Shutthanandan et al. (2004)], Ni [Zhu et al. (2006)], Mn and Fe [39] have been implanted in $TiO_2$ using low energy ion beam. Akdogan et al. (2006) observed a fraction of the Co ion has been implanted properly giving rise to a long range ferromagnetic order whereas the remaining Co exists as clusters showing

superparamgnetic behaviour. With a belief of dissolving Co clusters under annealing, Kim et al. (2005) heat treated the as implanted films at 900 °C under $1x10^{-6}$ Torr oxygen partial pressure. Few small Co clusters were found to dissolve inside the film but larger clusters were observed on the film surface that are composed of metallic Co confirmed by XMCD and XANES [Kim et al. (2005)]. However, Shutthanandan et al. (2004) could not able to see any Co/CoO phase in implanted films probed by element specific EXAFS and XANES. Instead of transition metals, ferromagnetism was also observed in single crystals of rutile $TiO_2$ by implanting inert ions like Ar/ N mediated by lattice defects [Cruz et al. (2009)]. Apart from magnetism, elements like Cr, V [Takeuchi et al. (2000)] and N [Nambu et al. (2006)] are also found to be implanted in $TiO_2$ for the possible photocatalytic applications.

***Irradiation in $TiO_2$***

SHIs were used to modify the structure of $TiO_2$ thin films by creating amorphized latent tracks/ point defects depending on the energy of the projectile ions [Ishikawa et al. (2006)]. Besides, amorphization of $TiO_2$, SHIs induced crystallization of amorphized titania to nanocrystalline phase [Thakurdesai et al. (2009)]. Structural phase transformation from anatase to rutile phase was observed with ion irradiation [Rath et al. (2009)]. Thakur et al. (2011) irradiated $TiO_2$ thin films form grown on α-$Al_2O_3$ (0001) substrates by rf-magnetron sputtering with 200 MeV $Ag^{15+}$ ions. With a fluence of $5x10^{12}$ ions/$cm^2$, anatase film showed ferromagnetism with phase converted to a mixed phase of rutile and brookite. The redistribution of charges among the Ti 3d and O 2p orbitals showed ferromagnetism, as evidenced from XMCD [Thakur et al. (2011)]. Rutile $TiO_2$ single crystals were irradiated with 2 MeV O ions at room temperature varying the fluence from 1 $x10^{15}$ to $5x10^{16}$ ions/$cm^2$. A $Ti^{3+}$-$O_V$ defect complex was generated due to ion irradiation. The $Ti^{3+}$ ions seemed to provide local 3*d* moments which are decisively related with the observed ferromagnetism. Also an optimum fluence was required to produce enough $Ti^{3+}$ ions keeping the crystalline ordering intact [Zhou et al. (2009)]. In case of

polycrystalline rutile target, implantation/irradiation of 4 MeV $^{40}Ar^{5+}$ ions also induced ferromagnetism due to oxygen vacancies [Sanyal et al. (2014)]. Hence use of ion beam causes controlled structural disorder that modifies the magnetic as well as electronic properties. In other sense one may use ion beams as a potential tool for defect engineering in materials science.

## 2.4 Discrepancies in Observed Ferromagnetism

The above experimental findings excite both experimentalists and theoreticians to comprehend the phenomena on the basis of various models (discussed in Chapter I). However, the exact origin of ferromagnetism in these systems is still complex and unclear. For example, samples produced in oxygen rich atmosphere show negligible magnetisation suggesting excess of oxygen as a factor that deteriorates the magnetism [Kim et al. (2002)]. Kim et al. (2005) and Shinde et al. (2004) noticed the presence of Co clusters in their samples leading to ferromagnetic order instead of intrinsic carriers mediating the magnetism. On the other hand, the experimental results obtained by Suryanarayanan et al. (2005) in Fe and Co-doped $TiO_2$ thin films highlighted the important role of oxygen vacancies driving the room temperature ferromagnetism in Fe/Co substituted $TiO_2$ films.

Recently, Ohtsuki et al. (2011) using the surface and bulk sensitive x-ray photoemission and XMCD measurements, experimentally demonstrated that ferromagnetism is mediated by Ti 3d electrons that couple the spins of Co atoms ferromagnetically as sketched in Fig.2.5 [Ohtsuki et al. (2011)]. In addition, the effect of electric field in switching the magnetisation is key issue for spintronic applications. Recently, Yamada et al. (2011) showed electric field induced room temperature ferromagnetism in Co-doped $TiO_2$. By applying a gate voltage of a few volts, a low-carrier paramagnetic state was transformed into a high-carrier ferromagnetic state revealing the significant role of electron carriers in these DMS materials [Yamada et al. (2011)].

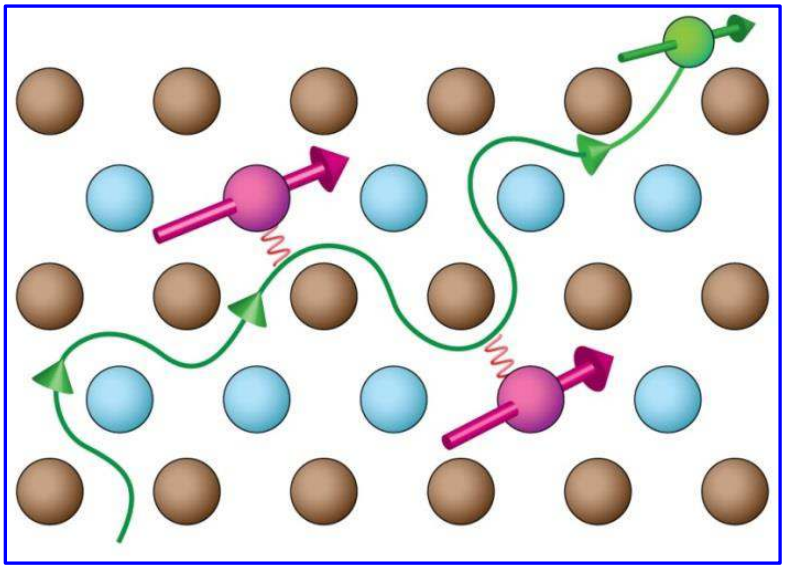

**Fig.2.5** A representation of a thin film of Co:$TiO_2$ in which ferromagnetism arises because titanium 3d electrons (green) travel around the material aligning the spin of cobalt atoms (pink) so that they all point in the same direction. The blue and brown spheres correspond to titanium and oxygen atoms, respectively. [After Ohtsuki et al. (2011)]

Though ferromagnetism has been reported by various workers, the reproducibility and lack of uniqueness of the observed magnetic moment has put the origin of magnetism suspicious. For example, 7at.% Co-doped $TiO_2$ in anatase form shown to have different magnetic moments like 0.32 $\mu_B$/Co [Matsumato et al. (2001)], 1.55 $\mu_B$/Co [Kim et al. (2003)] and 1.4 $\mu_B$/Co [Shinde et al. (2003)]. For the same 7% Co-doped $TiO_2$ in rutile form the moment is reported to be 1.75 $\mu_B$/Co [Hu et al. (2008)]. In case of nanoparticles, 7at.% Co-doped $TiO_2$ in anatase form have shown a decreased value of magnetic moment, i.e., 0.6 $\mu_B$/Co [Pereira et al. (2008)].

The various magnetic moment observed in the aforementioned reports suggest to understand the oxidation state of Co at Ti site. The oxidation state for substitutional Co must be +2. However, the ionic ground state of Co is debated. The two possibilities of $Co^{2+}$ with high spin ($3d^7$, $S$ = 3/2) [Kim et al. (2003)] or low spin ($3d^7$, $S$ = 1/2) [Chambers et al. (2001)] state is often raised (shown in Fig. 2.6). Looking at the wide spread of the observed magnetic moments, it really makes it tough to understand the exact ionic ground state of

Co. The formula used to calculate the spin-only magnetic moment ($\mu_{S.O}$) can be written as the number of unpaired electrons 'n' at the outermost orbital as:

$$\mu_{S.O} = \sqrt{n(n+2)}\,\mu_B$$

So magnetic moment of Co in high and low spin states are 3.87 $\mu_B$ and 1.73 $\mu_B$, respectively. However, these values are purely for metallic Co and most of the experimental results show magnetic moments that are less than these theoretically predicted values when Co is doped in $TiO_2$.

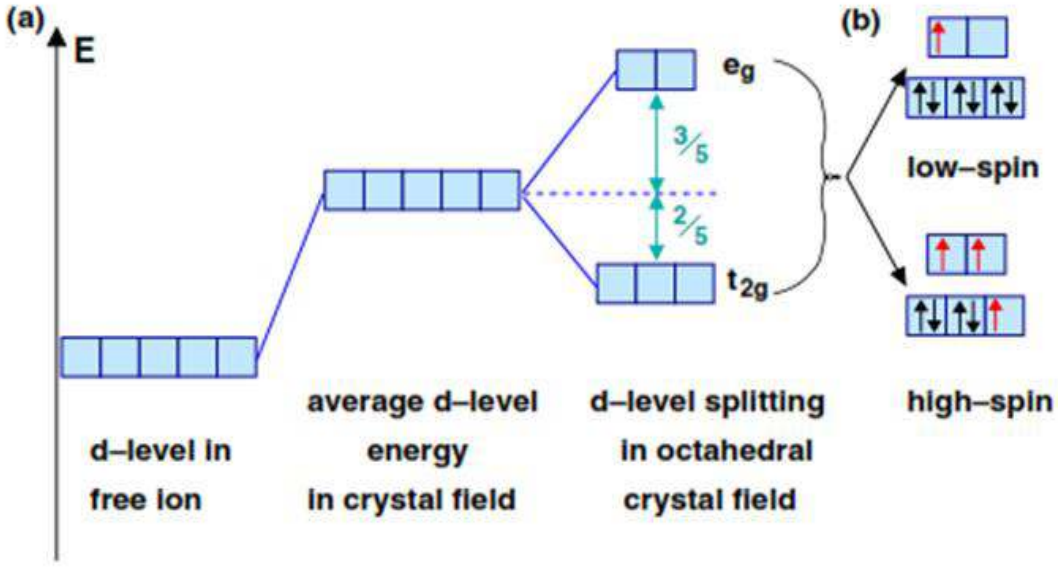


**Fig.2.6** (a) Splitting of d levels in an octahedral crystal field and (b) possible occupation schemes for a $Co^{2+}(3d^7 4s^0)$ atom. Unpaired spins are highlighted. [After Jannisch et al. (2005)]

Shinde et al. (2004) showed the clustering of Co atoms at the substrate and film interface for 2 at% Co-doped $TiO_2$ film deposited on R-$Al_2O_3$ substrates by PLD technique. The clustering of Co was clearly seen by cross-sectional TEM. Fig. 2.7 (a) shows the magnified image of the interface region as demarcated in Fig. 2.7 (b). The presence of Co at the bulk was also evidenced from magnetic and RBS measurements [Shinde et al. (2004)].

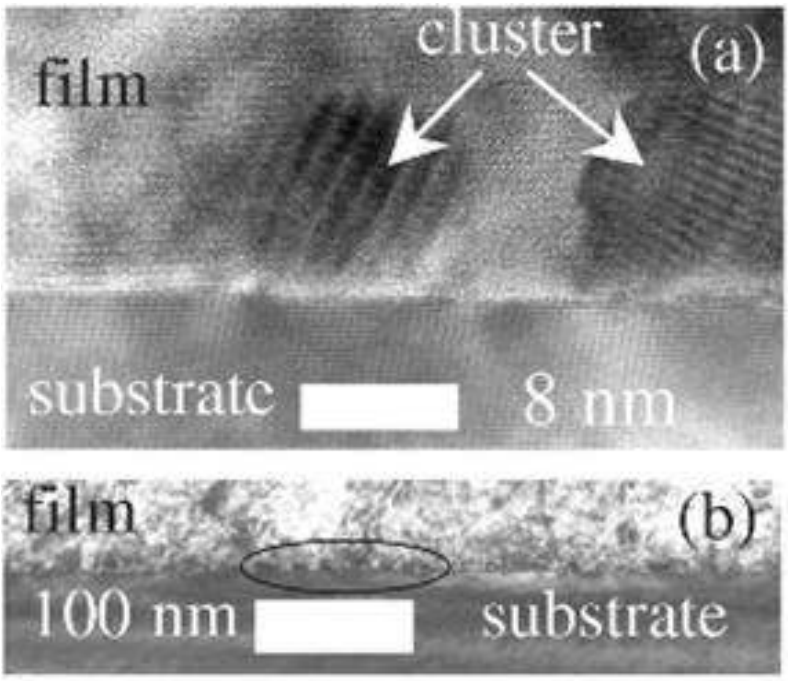


**Fig.2.7** TEM image of $Ti_{0.98}Co_{0.02}O_{2-\delta}$ film at different magnifications [After Shinde et al. (2004)]

Ohtsuki et al. (2011) studied the surface and bulk electronic properties of $Ti_{0.95}Co_{0.05}O_{2-\delta}$ thin films deposited by PLD on $SrTiO_3$ substrates using soft and hard x-ray photoemission spectroscopy using synchrotron radiation [Ohtsuki et al. (2011)]. The ferromagnetism in the sample was depicted by the hysteresis shown as inset of Fig.2.8 Hard x-ray PES and soft x-ray PES were measured with photon energies of 7940 and 1200 eV, respectively. The probe sensitivity for surface was 1 nm and ~ 10 nm for bulk. The zoomed view of the Ti $2p_{3/2}$ clearly shows the $Ti^{3+}$ component present in the bulk. XAS and RPES have revealed $Ti^{3+}$ electrons at Fermi level and high spin $Co^{2+}$ electrons occurring away from the Fermi level. Authors have suggested the condition for charge neutrality gave rise to the elusive Ti 3d carriers mediating ferromagnetism via Co 3d-O 2p-Ti 3d exchange interaction [Ohtsuki et al. (2011)].

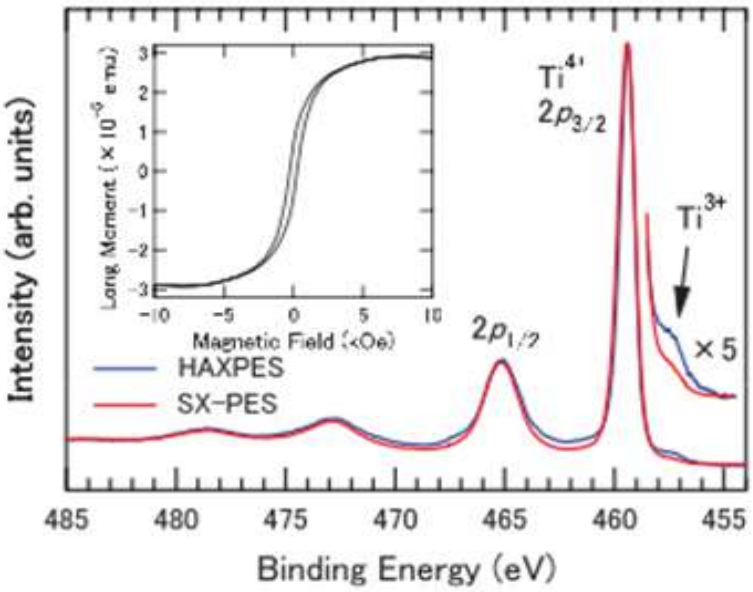


**Fig.2.8** Ti 2p core-level PES of Co:$TiO_2$ thin film by Hard x-ray PES (blue) and soft x-ray PES (red), respectively. The inset is the magnetisation vs magnetic field curve of the same film measured at room temperature. [After Ohtusuki (2011)]

Besides doping, it has been shown that extrinsic effects like unintentional incorporation of magnetic impurities during the course of sample handling with metallic (as considered non-magnetic stainless steel) spatulas and forceps can transfer magnetic impurities onto the sample before the sample is mounted for SQUID measurements. In addition, Teflon tapes or other plastic support used to mount the samples for SQUID measurement must be examined to ascertain the intrinsic ferromagnetic property of these DMS systems. Sometimes the contaminations of the as purchased substrates also give rise to ferromagnetism in the deposited films [Ogale (2010), Khalid et al. (2010), Yee et al. (2011)]. Earlier it was believed that observation of AHE is a true feature of intrinsic DMS property [Ramaneti et al. (2007)]. However, Shinde et al. (2004) observed the AHE in Co-doped $TiO_2$ thin films due to the presence of Co clusters.

Hence, from all these observations it is confirmed that the value of $T_C$, $M_S$, dopant solubility are not reproducible. Also there is no single experimental characterization technique is available to confirm the intrinsic DMS nature. However, one can only tailor the structural, magnetic or transport properties.

## 2.5 Objectives of the Present Thesis

Owing to the important role of defects like oxygen vacancies in the structural, electric and magnetic properties of the $TiO_2$, it is interesting to study its properties by controlling the defect concentration. The objectives of the present thesis are:

- To study the anatase to rutile transformation with size reduced to nano meter range, where the defect concentration is supposed to be very high. Also focus on the magnetic properties of Co doped $TiO_2$ nanoparticles.
- To study the microstructure and magnetic properties of $TiO_2$ nanowires synthesized by hydrothermal technique.
- To focus on the effect of oxygen partial pressure on structure and magnetic properties of $TiO_2$ and Co-doped $TiO_2$ (CTO) thin films deposited on Si and $LaAlO_3$ substrates. As the magnetism in such doped systems comes under the scanner regarding its intrinsic behaviour, one have to carefully explore the origin of magnetism avoiding any sorts of impurity contribution.
- To validate the universality of the ferromagnetism in nanostructured $TiO_2$ thin films grown on Si substrate by e-beam evaporation technique which has not been used for the magnetic study, with subsequent post-annealing in oxidizing as well as reducing atmospheres.
- To modify the structural and magnetic properties of $Ti_{1-x}Co_xO_{2-\delta}$ films after deposition with the help of swift heavy ion irradiation varying the ion fluence.
- To study the transport and magneto-transport properties of $Ti_{1-x}Co_xO_{2-\delta}$ films after ion irradiation.

The results of the present investigations are discussed in the subsequent chapters.